Two-mode Jahn-Teller effect in the absorption spectra of Fe^{2+} in II-VI and III-V semiconductors

O. Mualin and E. E. Vogel*
Departamento de Física, Universidad de La Frontera, Av. Francisco Salazar 01145, Casilla 54-D, Temuco, Chile

M. A. de Orúe
Departamento de Física, Universidad de Concepción, Casilla 160-C, Concepción, Chile

L. Martinelli and G. Bevilacqua
Dipartimento di Fisica, Università di Pisa, Piazza Torricelli 2, 56126, Pisa, Italy

H.-J. Schulz
Fritz-Haber-Institut der Max-Planck-Gessellschaft, Faradayweg 4-6, D-14195 Berlin, Germany
(Received 4 August 2001; published 27 December 2001)

Coupling of acoustical and optical modes is introduced to interpret zero-phonon lines in extended absorption spectra of Fe^{2+} in binary compounds of local symmetry T_d. Both cubic II-VI (CdTe, ZnTe, ZnSe, ZnS) and cubic III-V (GaAs, InP, GaP) compounds are included in analysis and calculations. For the case of ZnS:Fe^{2+}, which plays an important role here, interesting experiments are reported. The interpretation of the low-temperature absorption spectra of the seven systems unfolds generalities so all observed lines, as well as the absence of some expected lines, can be identified in the same generic way. In fact, only one parameter is freely varied, which is the coupling constant to one optical mode (additional to the usual acoustical one) which is necessary to explain high-energy lines. The general and consistent explanation of several lines for seven different systems provides a complete picture which allows a deep understanding of vibronic coupling to Fe^{2+} in binary compounds. The values of coupling constants explaining the experiments are tabulated.

DOI: 10.1103/PhysRevB.65.035211 PACS number(s): 71.70.Ej

I. INTRODUCTION

In the present paper we propose a consistent explanation for the low-temperature absorption spectra of Fe^{2+} as impurity substituting for the cation in the following seven zinc-blende crystals: CdTe,[1,2] ZnTe,[2,3] ZnSe,[2,4] ZnS,[1,5,6] GaAs,[6–8] InP,[6,9] GaP.[6,10] Additionally to this experimental information, we also include here our own absorption measurements for the case of ZnS:Fe^{2+}. This system seems to have all characteristics shown by most of the already mentioned spectra so it is important to discuss these features in the light of complete experimental information in ''clean'' samples and over an ample energy window.

The explanation of the zero-phonon lines ZPL's in these spectra requires the introduction of Jahn-Teller coupling.[11–14] In the past, several approaches have considered a few lines near the absorption edge. One of the most popular hypotheses is that one mode of symmetry ϵ suffices to cope with this phenomenon;[5,15,16] we will see that one acoustical mode is not capable of producing all observed ZPL's in the extended absorption range. It is also possible to try coupling τ_2 modes to the electronic orbitals present in Fe^{2+}.[17,18] Moreover, several authors have considered coupling to more than one phonon and also mixing ϵ and τ_2 modes.[19–22] Even more, multimode distributions have also been considered for this problem.[23] However, we will consider here coupling to ϵ modes only due to several reasons. Simplicity; if the experiment can be explained in a simple way there is no reason to bring in all other possible explanations which eventually have little weight. Interpretation; many modes mean many coupling constants allowing almost perfect numeric fits but obscuring physical interpretation. Consistency; since we will use an electronic Hamiltonian that neglects mixture to upper ionic levels and an elastic vibrational Hamiltonian, we need not invoke fine corrections in the coupling Hamiltonian. Effectiveness; the interesting features of the spectra to be explored here have more to do with considering acoustical and optical phonons than using several phonons of a kind.

To cope with calculations we have at our disposal three different methods, each one with appropriate computer algorithms.[24] This will allow precise numerical calculations in a way to be presented below. Our hypothesis is that all absorption spectra can be explained by the same Hamiltonian, handling a minimum number of parameters that take consistent values through the family of similar systems. The difference resides in the simultaneous explanation of the absorption spectra for seven systems in a broad energy window. We begin by considering the leading lines of each spectrum, covering next the entire absorption window. However, instead of tackling each compound as a separate case with its own Hamiltonian, we do a general analysis always with the same vibrational modes, thus reducing the variation of parameters to a minimum. We continue this analysis as to include a particular ZPL at about 200–300 cm^{-1} over the leading absorption line, which so far lacks a quantitative analysis. We will explain why this line is present in III-V compounds while it is only found in ZnS among the II-VI compounds. Finally, we will explain the existence of a broad structure found at a few hundred cm^{-1} over the threshold line.

We review experimental information in next section beginning by the analysis of our own absorption spectra on

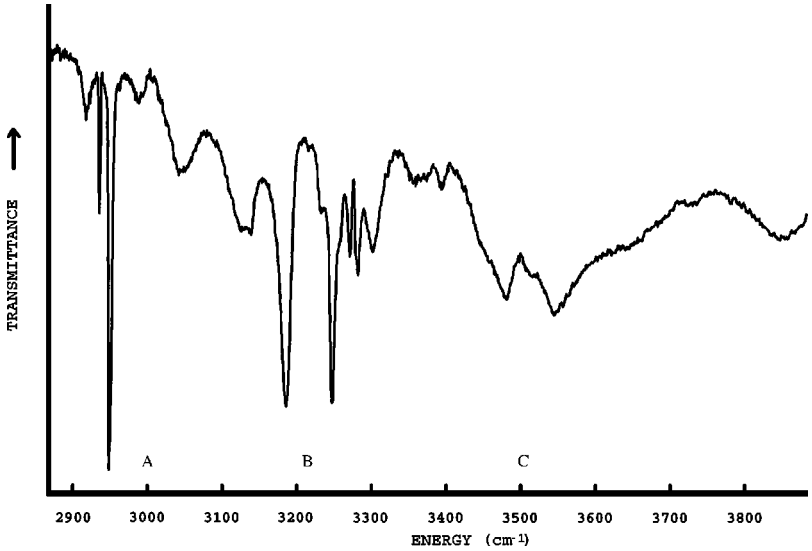

FIG. 1. Near-infrared transmission spectrum of sample 3094 (see text) at liquid-helium cooling in an immersion-type cryostat, recorded in lock-in technique by means of a conventional monochromator equipped with a cooled solid-state detector.

ZnS:Fe^{2+}. In Sec. III we define the Hamiltonian, approach, and scope for our calculations. In Sec. IV we present and comment on the most important results. Finally, in Sec. V we give several concluding remarks.

II. EXPERIMENT

Optical spectra of various ZnS:Fe crystals were recorded by conventional grating spectrometers (e.g., Jarrel-Ash) and by Fourier-transform spectroscopy (Bruker). Since crystals deliberately doped with iron usually display lack of definition in their spectral features, specimens containing iron impurities that entered unintentionally proved most useful for the present purpose. The high-resolution spectra in the range between 2900 and 4500 cm^{-1} obtained by both techniques at low temperatures ($T \cong 4$ K) turned out to be of comparable quality. In addition to the transmission curves presented here, photoluminescence spectra under different excitation conditions were studied for comparison purposes. We report below spectra on two different crystals. Crystal 3011 is a product of the former Aerospace Research Laboratories at Wright-Patterson AFB, Ohio. It was not intentionally doped. X-ray analysis shows some stacking faults. Crystal 3094 was grown in an iodine-transport procedure at the Technical University of Berlin. Besides a nominal doping by 10^{-3} mole Cr, traces of Ag, Mg, Si, and Mn have been detected. Judged from x-ray analysis and also by the structure of its optical spectra its crystal structure is preferentially cubic.

In Fig. 1 we present the absorption spectrum on sample 3094 taken by conventional spectroscopy at 4 K. A spectrum taken on sample 3011 also at 4 K by Fourier spectroscopy is entirely equivalent to the one presented in Fig. 1 so it will not be explicitly included here. The spectrum in Fig. 1 is similar to the three spectra reported by Slack and co-workers[1] with the following main differences: their line marked 1-7 is only barely visible in our spectra, while lines marked EX are not visible at all in the spectra reported here. Explanations for these facts were already anticipated in the just quoted paper. The line 1-7 is probably due to impurities occupying hexagonal sites, which are not present in equal amounts for different samples. The two lines denoted by EX were present only in one of the two samples measured in a previous work,[1] so they should not be attributed to Fe impurities. Indirectly, all of the above is a confirmation that the spectrum shown in Fig. 1 is due to iron impurities at cubic sites in our samples. So from now on we exclude from our analysis those three extra lines reported in previous experiments. We also took additional spectra at higher temperature on ZnS:Fe^{2+} samples; however, we do not include them explicitly here.

On the other hand, our spectra share several significant features with previous spectra, from which we mention here three, which are important for the present work. First, a second ZPL is present at about 40 cm^{-1} over the leading absorption line. Second, there is a clear ZPL in the intermediate region of the spectrum having a shoulder toward lower energies; such shoulder is activated by temperature due to absorption originating from levels γ_4, γ_3, etc. (see level scheme in Fig. 2). Third, there is a huge absorption structure in the approximate distance of 450–650 cm^{-1}. These three different regions in the spectrum allow a separation of lines according to energy ranges for a better discussion of results. Region A will include all clear ZPL close to the absorption threshold. Region B will be characterized by ZPL's in the middle of the spectrum showing thermal activation toward lower energies. Region C will include the high-energy absorption structure considered as a range not displaying possible individual lines. In this way we have constructed Table I, where the main readings from Fig. 1 are to be found at the central column in the second line of each box. In the first line of each box we give the same reading as taken from the paper of Slack and co-workers.[1] Spectrum presented by Podlowski *et al.* shows a general agreement with previous discussion although its resolution does not allow a more precise comparison.[6]

The information for other columns of Table I has been taken from the papers quoted therein having the same sequential order as in the main text. Not all cited spectra have the same resolution, so it is not always possible to single out all lines. Moreover, only some of them display all previously

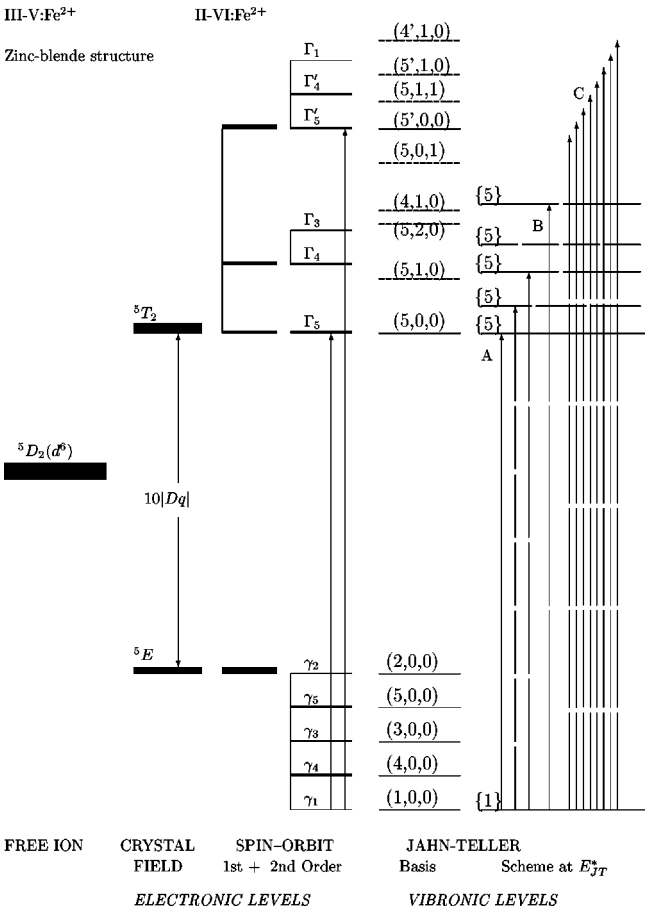

FIG. 2. Scheme of energy levels after considering successive interactions which are introduced from left to right. First, ionic multiplet $^5D_2$. Second, splitting due to crystalline field producing a separation $10|Dq|$ between the two components. Third, first-order spin-orbit interaction (leaving the ground multiplet unchanged). Fourth, splitting after second-order spin-orbit interactions: upward arrows illustrate the only two allowed absorptions (actually second one should be stronger). Fifth, formation of a vibronic basis for the excited multiplet in the Born-Oppenheimer limit: notation inside parentheses gives index of the representation, number of acoustical quanta, and number of optical quanta. Sixth, allowed low-temperature absorptions forming regions, A, B, and C defined in the text.

defined energy windows. In any case, the reader is referred to the original experimental work to better follow the discussion below. Energy differences are always referred to the leading or threshold absorption ZPL.

CdTe:Fe^{2+}. We begin with this system because it has the best defined structure for the low-energy lines (region A as defined above). In fact, it is the only system under consideration where it is possible to identify, without any doubt, up to five zero-phonon absorption lines. The threshold line occurs at 2282 cm^{-1}, followed by lines of similar or smaller intensities at approximate intervals of 12, 27, 36, and 52 cm^{-1}. From there on, all spectra of CdTe:Fe^{2+} are dominated by phonon-assisted transitions and regions B and C cannot be identified in a clear way. Apparently early measurements for CdTe and the other II-VI compounds reported below stressed the importance of region A over the rest of the spectrum.

ZnTe:Fe^{2+}. Spectra show the threshold line at 2490 cm^{-1}, followed by a well resolved ZPL at an interval near 12–15 cm^{-1}. Then a high and broad line is observed in the range 30–45 cm^{-1}; at least part of this absorption (if not all) should be attributed to the third ZPL which is expected to be always stronger than the second one.[24] There is no clear information for regions B and C.

ZnSe:Fe^{2+}. This system presents poorly resolved spectra. However, some similarities with the previous system allow us to read some of the lines. The threshold line is at 2747 cm^{-1}, followed by a second ZPL at a difference of 23 cm^{-1}, while the third line is broad as in previous case within the range 50–80 cm^{-1}. It is impossible to recognize the line for region B or the structure defining region C.

GaAs:Fe^{2+}. Threshold line occurs at 3002 cm^{-1}. The low-energy line close to the absorption threshold reported recently[8] is masked by the presence of lines α and $1a$ which were shown not to belong to Fe impurities. These extra lines are not present in other compounds analyzed here confirming their exotic origin. Fortunately, this energy region is resolved in a previously reported spectrum[7] which allows us to assign a weak ZPL at an interval of approximately 48 cm^{-1}. From there on, both experiments give similar results concerning a third broad line at about 90 cm^{-1}. No other clear possibility for a ZPL is to be seen in energy window A. However, the characteristic ZPL for region B is clearly found at 250 cm^{-1}. This feature can also be read in the spectrum of Podlowski *et al.*[6] Finally the broad structure forming region C appears in the range 450–500 cm^{-1}, narrower than in ZnS.

InP:Fe^{2+}. The absorption spectrum reported for this system is less resolved than the previous one. The threshold line at 2844 cm^{-1} is not followed by a second interval until we get to 72 cm^{-1}, which probably corresponds to the third line or structure; so there is no information on a second ZPL. The line for region B is clearly present at 273 cm^{-1}. However, the broad structure present in all other six compounds is less clear or not resolved.

GaP:Fe^{2+}. Spectra yield a threshold line at 3342 cm^{-1} followed by an ample and well resolved spectrum producing the first line at 54 cm^{-1}, followed by the usual broad line, this time centered around 113 cm^{-1}. The ZPL for region B is clear at 303 cm^{-1}. Then the structure for region C is very broad extending from 550–700 cm^{-1}.

Two of the common experimental facts shared by these systems have received little or none attention in the past: (i) The narrow ZPL for region B with thermal activity on the lower energy side; (ii) The broad structure toward the end of the absorption spectrum. For CdTe, ZnTe, and ZnSe as host crystals previous studies have concentrated on region A, since no clear line in region B or structure for region C have been characterized as such. On the other hand, when III-V compounds serve as host crystals the ZPL in region B is quite clear, and region C is well defined, while lines in region A are weaker or even lost as in the case of InP. This is where we can better appreciate the importance of the system ZnS:Fe^{2+}, showing activity in all three regions. This is the most important reason to include our results of Fig. 1 here.

TABLE I. Compilation of main absorption lines of Fe^{2+} in the host crystals heading columns. Main lines are included regardless of whether they are candidates for zero phonon lines or not. Threshold absorption line is given in terms of absolute values based on the most recent reference or measurement; second, third, and other lines in energy window A are given in terms of the relative differences Δ_2, Δ_3, . . . , with respect to threshold lines. Line in energy window B is labeled Δ_{11}. Range for lines forming the broad structure in energy window C is given under Δ_{21}. Double horizontal lines separate energy regions defined in the text. Measurements coming from different references are listed in separate lines (first reference goes in first line). Approximate representative values for $\hbar\omega$ for vibrational ϵ modes of host crystals are also given in the lower part (as read from the cited papers). Energy units in cm^{-1}. References correspond to those given in the main text; asterisk denotes experiment reported here in Fig. 1 and discussion in the text.

Description	CdTe (1,2)	ZnTe (2,3)	ZnSe (2,4)	ZnS (1)*	GaAs (7,8)	InP (9)	GaP (10)
Threshold (A)	2282	2490	2747	2948	3002	2844	3342
Δ_2 (A)	12	15	23	39	48	?	54
2nd Ref.		12		41	?		
Δ_3 (A)	27	30–45	50–80	104	91	72	113
2nd Ref.		30–45		100	90		
Δ_4 (A)	36						
2nd Ref.							
Δ_5 (A)	52						
2nd Ref.							
Δ_{11} (B)	?	?	?	296	250	273	303
2nd Ref.				300	250		
Δ_{21} (C)				450–650	450–500	?	550–700
2nd Ref.				450–650	450–500		
$\hbar\omega[TA(L)]$	30	40	50	75	60	55	80
$\hbar\omega[TA1(K)]$	35	55	70	90	85	75	105
$\hbar\omega[TA2(K)]$	50	75	100	120	110	115	150
$\hbar\omega(T0)$	140–160	170–190	230–270	300–350	250–270	310–340	330–370

An additional reason for this is to confirm the elimination of lines designated 1-7 and EX as already discussed above.

III. THEORY AND APPROACH

In a previous paper some of us presented three different methods to cope with Jahn-Teller calculations:[24] those of Born-Oppenheimer (BO),[15,25] Glauber (G),[26,27] and Lanczos (L).[28–30] More recently, we applied BO and L to explain the low-temperature luminescence spectra of Fe^{2+} in II-VI and III-V compounds.[31,32] We now apply these methods to explain the main features of the absorption spectra of Fe^{2+} in II-VI and III-V compounds. Since the coupling to acoustic phonons turns out to be at least of intermediate strength, BO is not appropriate to be used in the present analysis. On the other hand, L and G have been shown to agree for low and intermediate coupling ($S \leqslant 10$, as defined below), which we also verified for present systems. However, there is no reason to report equivalent results obtained by different methods thus including redundant information. Then, we will concentrate on results obtained after extensive use of L (easily implemented for a two-mode model) to explain the main features of the absorption spectra of Fe^{2+} in II-VI and III-V compounds. We will not discuss characteristics of individual methods here and the reader is kindly asked to look for them in the literature.[24]

Let us recall that Fe^{2+} presents a d^6 electronic configuration leading to a ^5D ground multiplet. Crystalline field very slightly mixes this level with upper ionic levels and, of prime relevance here, splits the ^5D multiplet into a ^5E ground level and a $^5T_2$ excited level, using group theory notation. Such splitting is illustrated on the left-hand side of Fig. 2. Spin-orbit coupling further splits these levels, leaving a γ_1 singlet as the true ground state, as shown in the central part of Fig. 2. At very low temperatures (liquid helium and below) only the level γ_1 is effectively populated. According to selection rules, electric-dipole absorptions originating from this state require final states of symmetry Γ_5. Plain crystal-field theory predicts two strong and sharp lines, separated by about 500 cm^{-1} represented by upward arrows in the central part of Fig. 2. The first line is always observed as the absorption threshold but the second sharp and strong line has never been observed as such in any of the seven compounds considered in Table I. Moreover, all the other lines and structures depicted in this table are not recognized by means of this simple approach.

Then, Jahn-Teller coupling is brought into the picture. From there on, vibronic states (in the extended Hilbert space produced by vibrational and electronic states) must be considered. The onset of such coupling is schematically shown toward the right-hand side of this figure by means of the notation $[\gamma, n_A, n_O]$: γ represents the symmetry of that level (γ_1 for the initial state and Γ_5 for the final states); n_A and n_O represent the number of acoustical and optical quantum numbers, respectively. Previous theoretical work has regarded only low-energy lines, explaining the first few lines close to

the threshold absorption. However, no attempt has been done to explain additional lines, in particular zones B and C of the spectra as previously discussed. This is one of the tasks of the present paper.

We avoid going into theoretical details here as they were recently presented elsewhere.[24] The total Hamiltonian comprises an electronic part H_e, a vibrational part H_v, and a coupling part H_{JT}. The electronic part includes all terms involving orbitals of the d^6 electrons (atomic up to spin-orbit terms and crystalline field). In all the analysis spin-orbit parameter λ is taken as $-100\ \mathrm{cm}^{-1}$, corresponding to the free ion value. The crystal-field parameter for each compound is adjusted to yield the appropriate absorption threshold using expressions including spin-orbit coupling in second-order perturbation theory.

The vibrational Hamiltonian H_v is considered in the elastic approximation by means of second quantization notation where a displacement is proportional to the sum of creation and annihilation operators. The coupling component depends on the hypothesis made with respect to coupling modes.

We stick to the idea of using modes of symmetry ϵ to couple to electronic orbitals of the impurity in what is usually referred to as $T_2 \otimes \epsilon$ coupling. Such local vibrational modes are produced by phonons belonging to points X and K of the Brillouin Zone (BZ).[5] So far, only acoustical phonons have been used to study this coupling. However, after thorough research we found that such an approach is incapable of producing the zero-phonon levels that are necessary to explain regions B and C of the spectra summarized in Table I. So we introduced coupling to optical phonons, additional to the acoustical one. In principle these modes also correspond to points X and K of the BZ, although the dispersion relations for optical modes are so flat, that this technical point loses relevance. Then the Jahn-Teller or vibronic Hamiltonian is written as

$$H_{JT}=K_A[(a^{\dagger}_{A\theta}+a_{A\theta})D_{\theta}+(a^{\dagger}_{A\epsilon}+a_{A\epsilon})D_{\epsilon}]+K_O[(a^{\dagger}_{O\theta}+a_{O\theta})D_{\theta}+(a^{\dagger}_{O\epsilon}+a_{O\epsilon})D_{\epsilon}], \quad (1)$$

with the usual definition of creation and annihilation operators for components θ and ϵ of an acoustical mode (index A) as well as an optical mode (index O). Normalized operators D for point group T_d have been tabulated by Koster *et al.*[33] Coupling constants K_A and K_O can be expressed as

$$K_A=\sqrt{E_{JTA}\hbar\omega_A}; \quad K_O=\sqrt{E_{JTO},\hbar\omega_O} \quad (2)$$

in terms of Jahn-Teller energies (E_{JT}) and frequencies (ω) of the corresponding coupling modes. Huang-Rhys factors S_A and S_O can be also defined:

$$S_A=\frac{E_{JTA}}{\hbar\omega_A}; \quad S_O=\frac{E_{JTO}}{\hbar\omega_O}. \quad (3)$$

Although the previous Hamiltonian has four parameters, in practice we will vary only one freely, while another one will be diminished slightly from previously established values with one-phonon coupling. Thus frequencies of the phonons, ω_A and ω_O, will be taken from lattice dynamics[34,35] within ranges summarized in Table I. Jahn-Teller energies for one acoustical phonon are known to be close to 200 cm^{-1} for II-VI compounds[15,16] so E_{JTA} will be varied around this value. So it is only E_{JTO} that will gradually increase in an ample range.

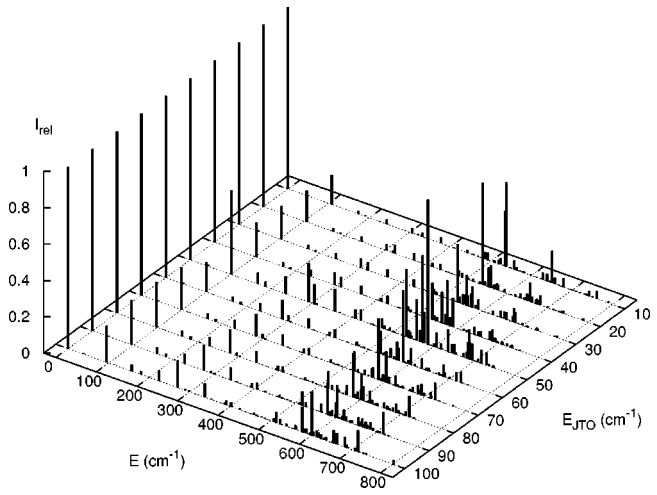

FIG. 3. Theoretical analysis for ZnS:Fe[2]. Phonon frequencies are kept fixed. Coupling to acoustical phonon is fixed at $E_{JTA}=190$ cm^{-1}. Coupling to optical mode is varied to follow variation of line close to 300 cm^{-1} (region B).

IV. RESULTS AND DISCUSSION

We begin our analysis by discussing ZnS:Fe^{2+} which is at the center of our presentation. From the discussion on parameters in the previous section and Table I, we choose $\hbar\omega_A=100\ \mathrm{cm}^{-1}$, and $\hbar\omega_O=340\ \mathrm{cm}^{-1}$. Previous work on II-VI compounds with one acoustical phonon was able to explain region A of the spectrum with $E_{JTA}\approx 230\ \mathrm{cm}^{-1}$. Upon introduction coupling to a second mode it is clear that the first coupling should decrease. We do so gradually as we increase E_{JTO} from nil to higher values. In Fig. 3 we present results obtained for $E_{JTA}=190\ \mathrm{cm}^{-1}$, varying E_{JTO} from 10 to 100 cm^{-1}. The position of each vertical line gives the calculated energy difference of each absorption with respect to the threshold, while the height is proportional to its intensity. Several consequences can be extracted from this figure. Weak coupling to optical modes does not change substantially the coupling to acoustical modes present in region A. The particular line in region B is a direct result from the presence of an optical phonon. This line in region B diminishes its energy and increases its intensity as E_{JTO} increases. Many lines appear over 500 cm^{-1} thus giving rise to an ample structure as observed in experiments. The distribution of lines within the structure is very sensitive to the strength of coupling to the optical mode.

According to experiments, a line in region B should be detected around 300 cm^{-1}. This value will be used to tune coupling to the optical mode. We found that $E_{JTO}\approx 55\ \mathrm{cm}^{-1}$, keeping all other parameters fixed at the values used in Fig. 3, describes the spectrum well. This is shown in the lower part of Fig. 4. The numerical values of energy and

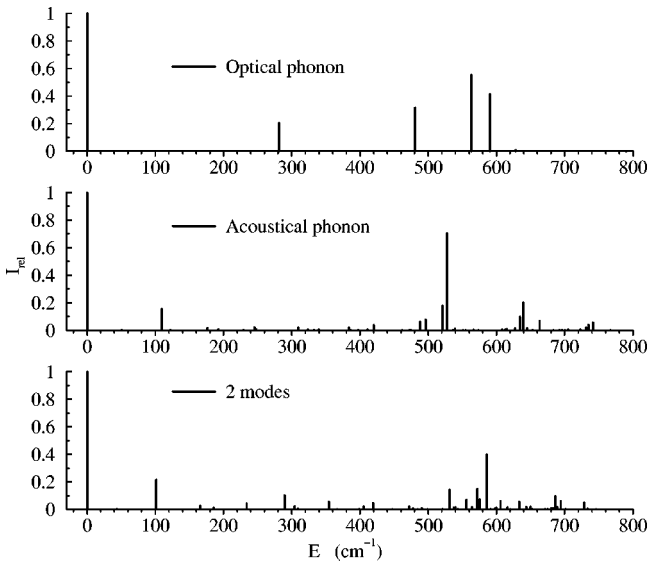

FIG. 4. Lower part represents the final fit for ZnS:Fe^{2+}, using the same parameters of Fig. 3 and fixing E_{JTO}=55 cm^{-1}. Intermediate part considers coupling to the acoustical phonon only. Upper part considers coupling to the optical phonon only. The succession of several closely packed absorption lines toward higher energies is due to both acoustical and optical phonons.

relative intensities are given in the central column of Table II. Aside from slight deviations of few percent the main features of the spectrum given in Fig. 1 are obtained. A second line ($\approx$40 cm^{-1}) can be observed in the experiments in spite of its low intensity because in this region there is no other source of absorption. The third line is clearly seen ($\approx$100 cm^{-1}), in a region where background and broadening is present due to phonon-assisted transitions. The line close to 300 cm^{-1} is there as already established by the tuning procedure. Then we realize that several important lines are found above 500 cm^{-1} thus explaining the broad structure in this region.

It is instructive to do a separate analysis for each coupling mode. In the intermediate portion of Fig. 4 we present vibronic levels resulting from considering coupling to the acoustical mode only: region B of the spectrum is completely lost. In the upper part of Fig. 4 we present results when only coupling to the optical mode is considered: now region A of the spectrum is lost. Moreover, in neither of these two partial analyses are enough levels of moderate intensity present above 500 cm^{-1} to produce the observed structure in region C. It is clear then that both modes are necessary to explain the main features of the absorption spectra of these systems in such a broad energy range as considered here.

Results for II-VI compounds. First we take phonon frequencies from the lattice dynamics summarized in Table I. Tuning for the other three II-VI compounds is not possible in the way done for ZnS. What we have done is to diminish E_{JTA} from values that adjust region A with one phonon, setting E_{JTO} to values that recover the explanation for region A of the experimental spectra. It is clear that this task can be achieved by a combination of values for E_{JTA} and E_{JTO}; it turns out that pairs of values for these magnitudes are very restricted in parameter space if a simultaneous explanation for several lines and intensities is to be achieved. Results for CdTe, ZnTe, and ZnSe using one suitable set of parameters tabulated in Table I are presented in Fig. 5. The agreement of calculations with the experimental spectra of CdTe, with five

TABLE II. Summary of calculated energy levels with Γ_5 components leading to zero-phonon absorptions. First row identifies host crystals following the same order as in the presentation of experimental results (Table I). Leading six rows give values of the four parameters used in the calculations reported in Figs. 4–6, according to the Hamiltonian defined in the text. Then energy differences with respect to the threshold line are reported for direct comparison to Table I. In parentheses we report relative intensities of absorptions ending in such level; in each column the threshold absorption is set to intensity 1.00. All lines with relative intensity larger than 0.01 are included; additionally we always include the second line. Energy units in cm^{-1}.

Host	CdTe	ZnTe	ZnSe	ZnS	GaAs	InP	GaP
$\hbar\omega_A$	35	50	70	100	85	75	105
E_{JTA}	210	220	210	190	160	170	180
S_A	6.0	4.20	3.00	1.90	1.88	2.27	1.71
$\hbar\omega_O$	150	180	250	340	260	320	350
E_{JTO}	30	30	40	55	40	60	50
S_O	0.20	0.17	0.16	0.16	0.15	0.19	0.14
Threshold	0.0 (1.00)	0.0 (1.00)	0.0 (1.00)	0.0 (1.00)	0.0 (1.00)	0.0 (1.00)	0.0 (1.00)
Δ_2	13 (0.99)	16 (0.04)	24 (0.03)	44 (0.01)	44 (0.02)	35 (0.001)	51 (0.01)
Δ_3	24 (0.73)	36 (0.96)	58 (0.33)	101 (0.22)	96 (0.14)	77 (0.19)	112 (0.19)
Δ_4	37 (0.33)	53 (0.10)	120 (0.05)	166 (0.03)	154 (0.02)		182 (0.03)
Δ_5	54 (0.26)	81 (0.24)	141 (0.02)	185 (0.01)	212 (0.03)	256 (0.04)	254 (0.04)
Δ_{11}	??	187 (0.06)	231 (0.05)	290 (0.10)	241 (0.13)	273 (0.11)	306 (0.14)
Δ_{12}	??	208 (0.01)	262 (0.03)	354 (0.06)	284 (0.02)		374 (0.05)
Δ_{13}		225 (0.03)	293 (0.01)	418 (0.05)			440 (0.06)

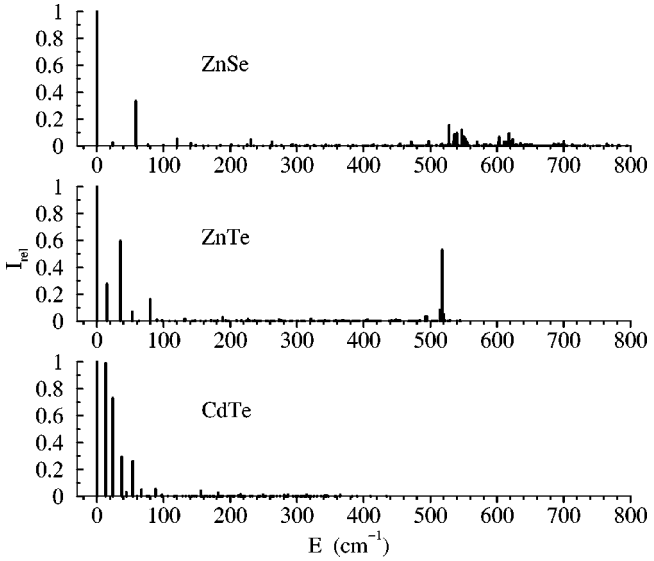

FIG. 5. Fit for the rest of the II-VI compounds (parameters are given in Table II). Line in region B is absent. Results for region C are uncertain due to lack of experimental information that can allow as to tune the optical mode.

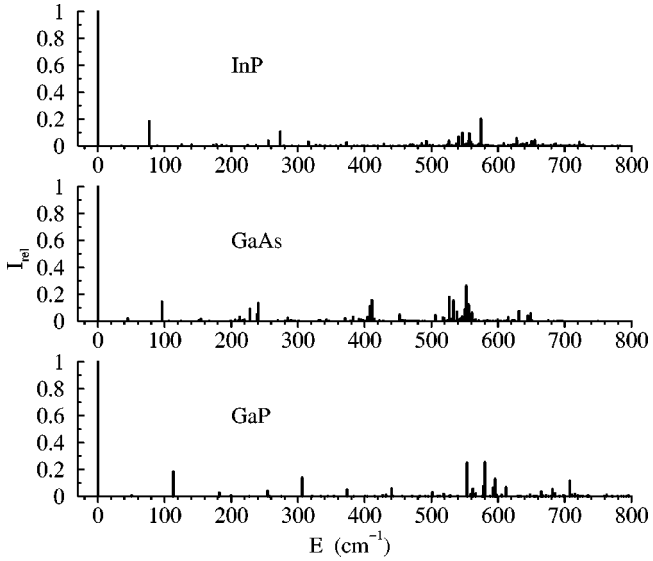

FIG. 6. Results for III-V compounds (parameters are given in Table II). Line in region B is very clear for GaAs and GaP, while it is weaker for InP. In any case, fine tuning is possible and the broad structure in region C emerges naturally for each system.

ZPL's in region A, is remarkable. Calculated spectra for ZnTe and ZnSe in this region also agree with experiments. The absence of lines in region B of the experimental spectra is also found in the three calculated spectra of Fig. 5. Actually, if larger coupling to optical modes is introduced the absent line in region B begins to show; this can also be interpreted as a test for an upper limit of coupling to the optical mode. However, nothing definite can be said for region C. In fact the distribution of possible lines to form this broad structure depends strongly on subtle changes in relative strength of the two couplings. Without the precise tuning mechanism used for ZnS is impossible at the moment to get beyond this point.

Results for III-V compounds. Here the analysis is done exactly as previously presented for ZnS, since in each case the ZPL of region B is well characterized. Calculated spectra for GaP, GaAs, and InP are presented in Fig. 6. The resemblance of these profiles with the corresponding experimental spectra is quite good. The absence of many ZPL in region A is well understood: larger phonon energies and lower JT coupling to acoustical modes weakens zero-phonon components in vibronic levels. The second line of region A is extremely weak and hard to detect (actually the spectrum of InP did not unfold the second line at all). The third line is stronger but at the same time broader since it is originally a two-phonon line. We continue to region B which is always clearly present and in agreement with observed spectra after the tuning done in each case. The broad structure toward higher energies (region C) deserves a special discussion since it is obtained directly by the previous procedure and without further tuning. In the case of GaP, experiments present the most extended structure of all these systems in the form of a double hump with the larger peak toward lower energies; this is roughly what can be observed in Fig. 6. In the case of GaAs the experiment gives a large structure just below 500 cm^{-1} with a shoulder toward lower energies; in our case we have the separate structures with the approximate right distribution of intensities. The absorptions corresponding to the shoulder are in agreement with the energies found in the experiment, but the larger portion of the structure is displaced by about 50 cm^{-1} to higher energies in our case. Finally, in the experiment for InP basically no broad structure is reported. In our calculations we can say that InP presents the weakest broad structure of all these compounds as it follows from Fig. 6. From this discussion flows quite clearly that the presence of such broad structure and its variety of shapes is due to a delicate balance between the coupling to acoustical and optical phonons.

V. CONCLUDING REMARKS

The main characteristics of the spectra of Fe^{2+} in II-VI and III-V compounds can be explained by a vibronic coupling including one acoustical and one optical phonon. Such coupling may produce a variety of ZPL's in three different regions of the low-temperature absorption spectrum.

The first few lines immediately above the absorption edge (region A) are due to coupling to acoustical phonons. Such coupling is more important for Fe^{2+} in II-VI compounds as compared to III-V compounds. For the former systems S_A is large (see Table II) in the intermediate level, approaching strong coupling in the case of CdTe. The only exception is ZnS, which is similar to III-V compounds where coupling is rather weak and these lines barely show in the spectra.

The next ZPL (region B) is due to coupling to optical modes. This coupling is weak and similar through all compounds ($S_O=0.1$ to $S_O=0.2$). However, it shows better for systems with larger optical frequencies since then it is possible to get a larger mixing of both Γ_5 and Γ_5' zero-phonon states producing one (and just one) vibronic level of symme-

try Γ_5 with an intermediate energy (200–300 cm^{-1}). This is so because the level Γ_5' has an energy intermediate between the vibronic levels originating from Γ_5 with one and two optical quanta. For systems with lower frequencies such superposition is not possible and electronic levels Γ_5 and Γ_5' lead to essentially uncoupled sets of vibronic levels. From Fig. 5 we see that ZnSe is a candidate for thorough investigation for a weak ZPL in region B.

The broad structure present in most of these systems a few hundred cm^{-1} over the first absorption line is due to both couplings. If any of them is turned off, such broad distribution of absorptions is replaced by a few intense peaks which have never been observed in these systems. On the contrary, if no coupling were present the strongest absorption line should be precisely one at an interval of 500 cm^{-1}. Coupling to any of the two phonons would break such sharp absorption into a few strong lines. It is only when simultaneous coupling to acoustical and optical phonons is invoked that many absorptions lines, close to each other, of low to moderate intensity show up.

Coupling to acoustical modes is stronger than coupling to optical modes. This finding stresses the importance of the overall polarization of the crystal on this coupling and not just the nearest neighbors which are strongly involved in the optical modes. It is also consistent with the larger values for E_{JT} reached for the more ionic II-VI compounds as can be seen in Table II.

Systems with low-frequency lattice dynamics spread zero-phonon components through several levels. This is one of the reasons for the relevance of region A in CdTe and region B in ZnS and the three III-V compounds. Toward region C a superposition of vibronic levels due to acoustical and optical modes coupled to both Γ_5 and Γ_5' levels produces a large admixture spreading absorption intensity through many vibronic levels losing individual intensity, but giving rise to a broad absorption.

ACKNOWLEDGMENTS

The following agencies and programs are acknowledged for partial support: FONDECYT (Chile) under Contract No. 1990875; International Collaboration CNR (Italy) and Conicyt (Chile); Millennium Nucleus "Condensed Matter Physics" (Mideplan Chile, P-99-135-F); Dirección de Investigación y Desarrollo Universidad de La Frontera; Dirección de Investigación Universidad de Concepción, MURST (Italy). Thanks are due to D. C. Reynolds, ARL, WPAB, and H.-J. Broschat, TUB, for the crystals, and to J. Nagel, G. Roussos, and M. Thiede for setting up experiments.

*Corresponding author. Fax: + 56 45 325323; Email address: evogel@ufro.cl

[1] G.A. Slack, F.S. Ham, and R.M. Chrenko, Phys. Rev. **152**, 376 (1966).
[2] J.M. Baranowski, J.W. Allen, and G.L. Pearson, Phys. Rev. **160**, 627 (1967).
[3] H.-J. Schulz, M. Thiede, U.W. Pohl, J. Rivera-Iratchet, M.A. de Orúe, M.L. Flores, O. Mualin, and E.E. Vogel, Z. Phys. B: Condens. Matter **98**, 215 (1995).
[4] J.H. Haanstra, in Proceedings of the International Conference on II-VI Semiconductor Compounds, edited by D.G. Thomas (Benjamin, New York, 1967), p. 207.
[5] F.S. Ham and G.A. Slack, Phys. Rev. B **4**, 777 (1971).
[6] L. Podlowski, R. Heitz, P. Thurian, A. Hoffmann, and I. Broser, J. Lumin. **58**, 252 (1994).
[7] G.K. Ippolitova and E.M. Omel'yanovskii, Sov. Phys. Semicond. **9**, 156 (1975).
[8] K. Pressel, G. Rückert, A. Dörnen, and K. Thonke, Phys. Rev. B **46**, 13 171 (1992).
[9] K. Pressel, K. Thonke, A. Dörnen, and G. Pensl, Phys. Rev. B **43**, 2239 (1991).
[10] G. Rückert, K. Pressel, A. Dörnen, K. Thonke, and W. Ulrici, Phys. Rev. B **46**, 13 207 (1992)
[11] H.A. Jahn and E. Teller, Proc. R. Soc. London, Ser. A **161**, 220 (1937).
[12] R. Englman, The *Jahn-Teller Effect in Molecules and Crystals* (Wiley-Interscience, New York, 1972).
[13] I. B. Bersuker, The *Jahn-Teller Effect and Vibronic Interactions in Quantum Chemistry* (Plenum, New York, 1984).
[14] *Proceedings of the XIV International Symposium on Electron Phonon Dynamics and The Jahn-Teller Effect*, edited by G. Bevilacqua, L. Martinelli, and N. Terzi (World-Scientific, Singapore, 1999).
[15] J. Rivera-Iratchet, M.A. de Orúe, and E.E. Vogel, Phys. Rev. B **34**, 3992 (1986).
[16] E.E. Vogel, J. Rivera-Iratchet, and M.A. de Orúe, Phys. Rev. B **38**, 3556 (1988).
[17] V. Savona, F. Bassani, and S. Rodriguez, Phys. Rev. B **49**, 2408 (1994).
[18] D. Colignon, E. Kartheuser, S. Rodriguez, and M. Villeret, Phys. Rev. B **51**, 4849 (1995).
[19] L. Martinelli, M. Passaro, and G. Pastori Parravicini, Phys. Rev. B **40**, 10 443 (1989).
[20] D. Colignon and E. Kartheuser, Z. Phys. Chem. (Munich) **201 S**, 119 (1997).
[21] D. Colignon, Ph.D. thesis, Université de Liege, 1998.
[22] D. Colignon, E. Kartheuser, S. Rodriguez, and M. Villeret, Phys. Rev. B **51**, 4849 (1995).
[23] A.I. Ryskin, Opt. Spectrosc. **78**, 846 (1995).
[24] L. Martinelli, G. Bevilaqcua, J. Rivera-Iratchet, M.A. de Orúe, O. Mualin, E.E. Vogel, and J. Cartes, Phys. Rev. B **62**, 10 873 (2000).
[25] H. Maier and U. Scherz, Phys. Status Solidi B **62**, 153 (1974).
[26] B.R. Judd and E.E. Vogel, Phys. Rev. B **11**, 2427 (1975).
[27] J. Rivera-Iratchet, M.A. de Orúe, M.L. Flores, and E.E. Vogel, Phys. Rev. B **47**, 10 164 (1993).
[28] R. Haydock, V. Heine, and M.J. Kelly, J. Phys. C **5**, 2845 (1972).
[29] G. Grosso and G. Pastori Parravicini, Adv. Chem. Phys. **62**, 133 (1985).
[30] G. Grosso, L. Martinelli, and G. Pastori Parravicini, Phys. Rev. B **51**, 13 033 (1995).
[31] E.E. Vogel, O. Mualin, H.-J. Schulz, and M. Thiede, Z. Phys. Chem. (Munich) **201 S**, 99 (1997).
[32] G. Bevilaqcua, L. Martinelli, G. Russo, G. Pastori Parravicini, O. Mualin, E.E. Vogel, M.A. de Orúe, and J. Rivera-Iratchet, in

Vibronic Interactions: Jahn-Teller Effects in Crystals and Molecules, edited by M. Kaplan and G. Zimmerman, NATO Science Series, II. Mathematics, Physics Chemistry (Kluwer Academic, Dordrecht, 2001), Vol. 39, pp. 377–380.

[33] G.F Koster, J.O Dimmock, R.G. Wheeler, and H. Statz, *Properties of the Thirty-Two Point Groups* (MIT University Press, Cambridge, MA, 1963).

[34] T. Soma and H. Matsuo Kagaya, Solid State Commun. **46**, 773 (1983).

[35] H.-Matsuo Kagaya and T. Soma, Phys. Status Solidi B **124**, 37 (1984).